Anti-Inflammatory Mechanisms in Mice

19. Scientific Sessions 2013 of the American Heart Association (November 16-20 2013, Dallas) Antoku Y, Matoba T, Yufu T, Nakano K, Sunagawa K, Egashira K: A Novel Rabbit Model of Plaque Erosion with Spontaneous Atherothrombotic Occlusion

20. Scientific Sessions 2013 of the American Heart Association (November 16-20 2013, Dallas) Ikeda G, Matoba T, Nakano Y, Nagaoka K, Nakano K, Sunagawa K, Egashira K: Nanoparticle-Mediated Targeting of Cyclosporine A to Mitochondria in Reperfused Myocardium Enhances Cardioprotection from Ischemia-Reperfusion Injury

21. Scientific Sessions 2013 of the American Heart Association (November 16-20 2013, Dallas) Ichimura K, Nakano K, Nagaoka K, Matoba T, Egusa S, Sunagawa K, Egashira K: Nanoparticle-Mediated Targeting of Pitavastatin into Reperfused Myocardium Reduces Ischemia-Reperfusion Injury in a Preclinical Pig Model

（3）出版物

＜総説＞

1. 香月俊輔、的場哲哉、中野覚、古賀純一郎、江頭健輔：特集　炎症・免疫からみた心血管病　不安定プラークと炎症．循環器内科　科学評論社　2011；69(6)：547-552

2. 中野覚、江頭健輔：「血管内皮細胞選択的ナノ DDS 技術」を活用した低侵襲ナノ医療の開発．臨床評価　臨床評価刊行会　2011；39(2)：300-304

3. 中野覚、由布威雄、江頭健輔：ナノ DDS デバイスを用いた血管内治療の臨床応用．Drug Delivery System　日本 DDS 学会　2012; 27(4): 275-282

4. 的場哲哉、江頭健輔：ナノ粒子 DDS を用いた血管新生治療法の開発　Bio Clinica 北隆館　2013；28（5）：35-39

5. 香月俊輔、的場哲哉、江頭健輔：ナノ粒子を用いた新規 Drug Delivery System (DDS)によるプラーク不安定化，破綻治療．Heart View　メジカルビュー社　2013；17(4)：76(408)-84(416)

6. 江頭健輔、中野覚：シーズ成果報告〈医薬品〉急性心筋梗塞症治療用ナノ粒子製剤の実用化のための橋渡し研究．臨床評価　臨床評価刊行会　2013；41(1)：68-71

7. 江頭健輔、中野覚、松本拓也、前原喜彦：シーズ成果報告〈医薬品〉虚血肢治療用低侵襲ナノ粒子製剤の実用化．臨床評価　臨床評価刊行会　2013；41(1)：

72-74

＜著書＞

1. 江頭健輔、的場哲哉：ナノテクノロジー　血管生物医学事典　血管生物医学会 2011；435-436

2. 中野覚、江頭健輔：第２章　徐放技術の医療応用　４．新規治療　８）ナノ DDS ステントを用いた血管内治療の臨床への応用．ここまで広がるドラッグ徐放技術の最前線　古くて新しいドラッグデリバリーシステム(DDS)　メディカル ドゥ　2013；240-245

＜新聞報道＞

1. 平成 23 年 08 月 01 日掲載、日本経済新聞 「ナノ DDS 技術による革新的低侵襲治療的血管新生療法の橋渡し研究」について、24 年度に医師主導型治験を開始する旨が掲載。

2. 平成 25 年 5 月 19 日掲載、首相官邸ホームページ「佐賀県及び福岡県下訪問」

3. 平成 25 年 5 月 19 日掲載、毎日新聞「安倍首相：九州の最先端治療設備を視察」

4. 平成 25 年 5 月 19 日掲載、msn 産経ニュース「『私自身も難病に苦しんだ』首相が先端医療の現場視察」

5. 平成 25 年 5 月 19 日掲載、朝日新聞 「安倍首相、先端医療の輸出強調　九州視察で成長戦略説く」

6. 平成 25 年 5 月 20 日掲載、産経新聞「難病治療『私の天命』首相、九大病院を視察」

【研究成果の刊行物・別刷】

○をつけた論文の別刷あるいは資料を次のページ以降に添付します。

Nanoparticle-Mediated Delivery of Pitavastatin Inhibits Atherosclerotic Plaque Destabilization/Rupture in Mice by Regulating the Recruitment of Inflammatory Monocytes

Shunsuke Katsuki, MD; Tetsuya Matoba, MD, PhD; Soichi Nakashiro, MD; Kei Sato, PhD; Jun-ichiro Koga, MD, PhD; Kaku Nakano, PhD; Yasuhiro Nakano, MD; Shizuka Egusa, PhD; Kenji Sunagawa, MD, PhD; Kensuke Egashira, MD, PhD

Background—Preventing atherosclerotic plaque destabilization and rupture is the most reasonable therapeutic strategy for acute myocardial infarction. Therefore, we tested the hypotheses that (1) inflammatory monocytes play a causative role in plaque destabilization and rupture and (2) the nanoparticle-mediated delivery of pitavastatin into circulating inflammatory monocytes inhibits plaque destabilization and rupture.

Methods and Results—We used a model of plaque destabilization and rupture in the brachiocephalic arteries of apolipoprotein E–deficient ($ApoE^{-/-}$) mice fed a high-fat diet and infused with angiotensin II. The adoptive transfer of $CCR2^{+/+}$Ly-$6C^{high}$ inflammatory macrophages, but not $CCR2^{-/-}$ leukocytes, accelerated plaque destabilization associated with increased serum monocyte chemoattractant protein-1 (MCP-1), monocyte-colony stimulating factor, and matrix metalloproteinase-9. We prepared poly(lactic-co-glycolic) acid nanoparticles that were incorporated by Ly-$6G^{-}CD11b^{+}$ monocytes and delivered into atherosclerotic plaques after intravenous administration. Intravenous treatment with pitavastatin-incorporated nanoparticles, but not with control nanoparticles or pitavastatin alone, inhibited plaque destabilization and rupture associated with decreased monocyte infiltration and gelatinase activity in the plaque. Pitavastatin-incorporated nanoparticles inhibited MCP-1–induced monocyte chemotaxis and the secretion of MCP-1 and matrix metalloproteinase-9 from cultured macrophages. Furthermore, the nanoparticle-mediated anti–MCP-1 gene therapy reduced the incidence of plaque destabilization and rupture.

Conclusions—The recruitment of inflammatory monocytes is critical in the pathogenesis of plaque destabilization and rupture, and nanoparticle-mediated pitavastatin delivery is a promising therapeutic strategy to inhibit plaque destabilization and rupture by regulating MCP-1/CCR2–dependent monocyte recruitment in this model. **(*Circulation*. 2014;129:896-906.)**

Key Words: monocytes ■ myocardial infarction ■ nanoparticles ■ plaque ■ statins, HMG-CoA

Coronary heart disease is the leading cause of death worldwide, and at least 7 million patients die of this disease each year (386 324 people in the United States alone).[1] Acute myocardial infarction (AMI) is the most severe type of coronary heart disease and the most frequent cause of heart failure, and it impairs the quality of life and inflates medical costs. Timely and successful revascularization therapy for AMI reduces short-term mortality, and current standard medical therapy with angiotensin-converting enzyme inhibitors and β-blockers ameliorates the development of post–myocardial infarction heart failure. However, these recent advances in therapeutic intervention for AMI are associated with an increased prevalence of heart failure with high long-term mortality, which remains a serious concern.[2] In the United States, 5.1 million people experienced heart failure in 2010, and 274 601 people died of heart failure in 2009.[1] Therefore, there is an urgent need for preventive treatment to avoid plaque destabilization and rupture, which directly cause AMI.

Clinical Perspective on p 906

Rupture-prone unstable atherosclerotic plaques feature monocyte/macrophage infiltration, lipid core formation, and fibrous cap thinning by matrix metalloproteinases (MMPs).[3] Recent reports suggest that monocytes are functionally polarized into at least 2 major subsets: Inflammatory monocytes ($CD14^{++}CD16^{-}$ in humans and Ly-$6C^{high}CCR2^{+}CX3CR1^{low}$ in mice) and anti-inflammatory monocytes ($CD14^{+}CD16^{+}$ in humans and Ly-$6C^{low}CCR2^{-}CX3CR1^{high}$ in mice).[4] Inflammatory monocytes are found in the peripheral blood of patients with AMI,[5]

Received April 2, 2013; accepted November 15, 2013.

From the Department of Cardiovascular Medicine (S.K., T.M., S.N., J.K., Y.N., S.E., K. Sunagawa) and Department of Cardiovascular Research, Development, and Translational Medicine (K. Sato, K.N., K.E.), Kyushu University Graduate School of Medical Sciences, Fukuoka, Japan.

The online-only Data Supplement is available with this article at http://circ.ahajournals.org/lookup/suppl/doi:10.1161/CIRCULATIONAHA.113.002870/-/DC1.

Correspondence to Kensuke Egashira, MD, PhD, FAHA, Department of Cardiovascular Research, Development, and Translational Medicine, Kyushu University Graduate School of Medical Sciences, 3-1-1 Maidashi, Higashi-ku, Fukuoka 812-8582, Japan. E-mail egashira@cardiol.med.kyushu-u.ac.jp

Circulation **is available at http://circ.ahajournals.org** **DOI: 10.1161/CIRCULATIONAHA.113.002870**

which suggests that they have a pathological role in plaque destabilization; however, substantial proof for a causative role of inflammatory monocytes in the pathogenesis of plaque destabilization and rupture is lacking.

HMG-CoA reductase inhibitors (statins) lower serum cholesterol levels and reduce cardiovascular events and mortality by 32% to 37% in primary prevention trials[6,7] and 24% to 30% in secondary prevention trials.[8,9] Data from clinical trials indicate that although the intensive use of statins reduces serum C-reactive protein levels and cardiovascular risk and attenuates the progression of coronary artery plaque,[10–13] the risk reduction caused by on-label doses of statins remains insufficient to suppress AMI.[10] In animals, plaque-stabilizing effects have been observed after high doses of statins.[14–18] Statins exert multiple vasculoprotective effects on endothelial cells, vascular smooth muscle cells, and monocytes.[19–21] Thus, we hypothesized that the controlled delivery of statins to inflammatory monocytes and atherosclerotic plaques might optimize the plaque-stabilizing effects of statins.

Recently, we developed a novel nanoparticle-mediated drug-delivery system (DDS) that is formulated from bioabsorbable poly(lactic-co-glycolic) acid (PLGA) polymer, and we reported that nanoparticles were taken up by a variety of cells, such as monocytes, vascular smooth muscle cells, and endothelial cells. In addition, the nanoparticle-mediated DDS showed a significant enhancement in the therapeutic effects on ischemia-induced neovascularization[22,23] and pulmonary arterial hypertension[24] in animal models compared with conventional administration. Nanoparticles are rapidly taken up by circulating monocytes and the mononuclear phagocytic system after intravenous administration,[25] and nano-sized contrast agents accumulate in atherosclerotic plaques.[26] To the best of our knowledge, no prior studies have addressed whether polymeric nanoparticles accumulate in unstable atherosclerotic plaques after intravenous administration or whether the nanoparticle-mediated delivery of pitavastatin has therapeutic effects on plaque destabilization and rupture in vivo. Therefore, we tested the hypotheses that (1) inflammatory monocytes play a causative role in plaque destabilization and rupture and (2) the nanoparticle-mediated delivery of pitavastatin inhibits plaque destabilization and rupture by targeting inflammatory monocytes.

Methods

Experimental Animals

Male apolipoprotein E–deficient ($ApoE^{-/-}$) mice on the C57BL/6J genetic background were purchased from Jackson Laboratory (Bar Harbor, ME). $ApoE^{-/-}CCR2^{-/-}$ and $ApoE^{-/-}CCR2^{+/+}$ mice with the same genetic background (C57BL/6J and 129/svjae hybrids) were used.[27] Animals were maintained on a 12-hour light-dark cycle with free access to normal rodent chow and water.

Diet Preparation

A high-fat diet that contained 21% fat from lard and was supplemented with 0.15% (wt/wt) pure cholesterol (Oriental Yeast, Tokyo, Japan) was prepared according to the formula recommended by the American Institute of Nutrition. Additional details can be found in the online-only Data Supplement.

Experimental Protocol

The study protocol was reviewed and approved by the Committee on the Ethics of Animal Experiments, Kyushu University Graduate School of Medical Sciences. The 4 sets of animal experiments are depicted in a schematic in Figure I in the online-only Data Supplement). Brachiocephalic arteries were isolated with the aortic arches. Isolated samples were fixed in 3.7% formaldehyde for histological and immunohistochemical analyses or were snap-frozen in liquid nitrogen and stored at −80°C for biochemical analysis. Additional details for each experimental protocol can be found in the online-only Data Supplement.

Histopathology and Immunohistochemistry

Histopathological and immunohistochemical evaluations were performed to quantify atherosclerosis and examine both plaque morphology and the mechanism of plaque destabilization and rupture. Atherosclerotic plaques were stained with oil red O, and cross sections of the brachiocephalic arteries and aortic root were stained with elastica van Gieson, antimacrophage surface glycoprotein Mac3, and monocyte chemoattractant protein-1 (MCP-1). Additional details are provided in the online-only Data Supplement.

Flow Cytometry

Leukocytes from peripheral blood and the spleen and peritoneal cells were obtained from mice and analyzed with a FACSCalibur cytometer (Becton-Dickinson Biosciences, San Jose, CA). Additional details can be found in the online-only Data Supplement.

Preparation of PLGA Nanoparticles

PLGA nanoparticles encapsulated with FITC (FITC-NP), pitavastatin (pitavastatin-NP) and 7ND plasmid (7ND-NP) were prepared by use of an emulsion solvent diffusion method, as reported previously.[22–24] Additional details can be found in the online-only Data Supplement.

In Vivo Kinetics of the Nanoparticles

Excised aortas from the atherosclerotic mice were intravenously injected with or without FITC-NP and were evaluated by stereoscopic and fluorescence microscopy. Sections of the brachiocephalic artery were evaluated by fluorescence microscopy or were stained with hematoxylin and eosin. Additional details can be found in the online-only Data Supplement.

In Situ Zymography

Gelatinase (MMP-2/gelatinase-A and MMP-9/gelatinase-B) activity was measured in unfixed frozen sections with quenched fluorescein-labeled gelatinase substrate (DQ gelatin; Invitrogen, Eugene, OR).[28] Additional details can be found in the online-only Data Supplement.

Gelatin Zymography

The lipopolysaccharide-induced gelatinase activity of RAW264.7 cells was measured with a gelatin Zymo electrophoresis kit (Primary Cell, Hokkaido, Japan) according to the manufacturer's directions. Additional details can be found in the online-only Data Supplement.

Real-Time Quantitative Reverse-Transcription Polymerase Chain Reaction

Real-time polymerase chain reaction amplification was performed with mouse cDNA with the use of the ABI PRISM 7000 sequence detection system (Applied Biosystems/Life Technologies, Carlsbad, CA), as described previously.[29] The polymerase chain reaction primers and TaqMan probes we used can be found in the online-only Data Supplement.

Chemotaxis Assay

The chemotactic activity of THP-1 cells in response to MCP-1 was measured by a Boyden chamber method, as described previously.[30] Additional details can be found in the online-only Data Supplement.

Statistical Analysis

Data are expressed as mean±SE. For analysis of the number of buried/disrupted fibrous caps, differences were analyzed statistically by ANOVA followed by the Dunn multiple comparison test, and differences between 2 groups were analyzed with the Mann-Whitney test. For the other analyses, differences were analyzed statistically by ANOVA followed by post hoc Bonferroni or Dunnett multiple comparison tests. Differences between 2 groups were analyzed with an unpaired *t* test. $P<0.05$ was considered significant.

Results

Adoptive Transfer of Inflammatory Macrophages Accelerated Plaque Destabilization and Rupture

To clarify the role of inflammatory monocyte/macrophages in plaque destabilization and rupture, we first examined whether the adoptive transfer of inflammatory macrophages accelerates plaque destabilization and rupture in a murine model. We collected thioglycollate-induced peritoneal leukocytes from ApoE$^{-/-}$CCR2$^{+/+}$ mice that contained Ly-6C^{high} inflammatory macrophages and from ApoE$^{-/-}$CCR2$^{-/-}$ mice that contained <5% inflammatory macrophages (Figure IIA and IIB in the online-only Data Supplement).[4,31] ApoE$^{-/-}$ mice were assigned to the no-treatment group, the CCR2$^{+/+}$ inflammatory macrophage group (1×10^6 peritoneal leukocytes from ApoE$^{-/-}$CCR2$^{+/+}$ mice), or the CCR2$^{-/-}$ leukocyte group (1×10^6 peritoneal leukocytes from ApoE$^{-/-}$CCR2$^{-/-}$ mice). The adoptive transfer of CCR2$^{+/+}$ inflammatory macrophages tended to increase the incidence of disrupted/buried fibrous caps. The adoptive transfer of CCR2$^{-/-}$ leukocytes significantly decreased the incidence of disrupted/buried fibrous caps compared with that of CCR2$^{+/+}$ inflammatory macrophages (Figure 1A; Table 1). These results demonstrate that inflammatory macrophages responsible for plaque rupture are recruited from the circulation via MCP-1/CCR2 signaling, which suggests a role for peripheral Ly-6C^{high} monocytes as the precursor of inflammatory macrophages. Because splenic monocytes show a phenotype comparable to that of peripheral monocytes,[32] we purified splenic monocytes from ApoE$^{-/-}$ mice fed a high-fat diet and examined whether the adoptive transfer of splenic monocytes accelerated plaque destabilization and rupture in the same model. We confirmed ≈90% purity of splenic monocytes after negative selection using magnetic cell separation, ≈85% of which expressed a high level of Ly-6C (Figure IIIA in the online-only Data Supplement). Consistent with the data from the adoptive transfer of CCR2$^{+/+}$ peritoneal macrophages, the adoptive transfer of splenic monocytes tended to increase the incidence of disrupted/buried fibrous caps ($P=0.056$; Figure IIIB in the online-only Data Supplement), which confirms the detrimental role of inflammatory monocyte/macrophage lineage in atherosclerotic plaque rupture (Figure IIIB in the online-only Data Supplement).

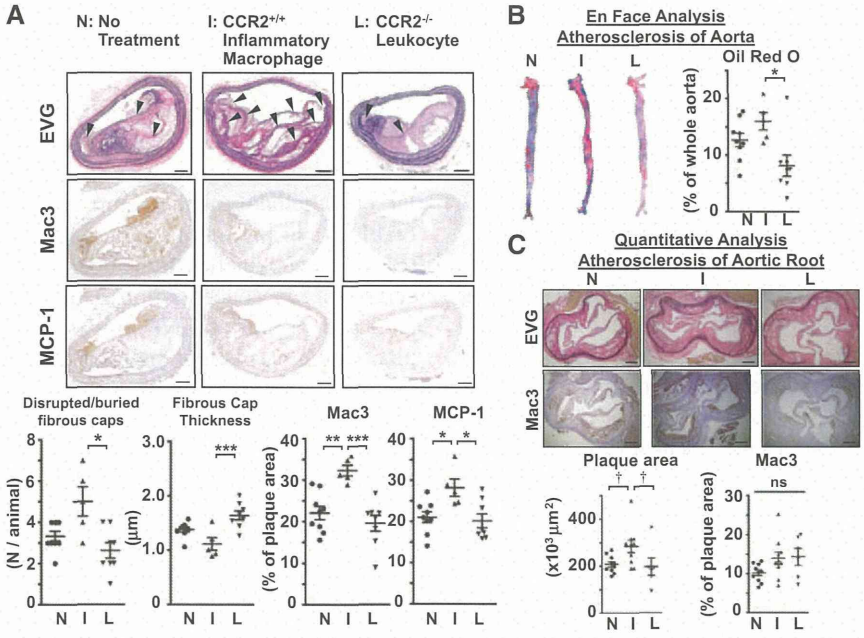

Figure 1. The adoptive transfer of inflammatory macrophages accelerated plaque destabilization and rupture. **A**, **Top**, Photomicrographs of atherosclerotic plaques in the brachiocephalic artery stained with elastica van Gieson (EVG), the antimacrophage surface glycoprotein Mac3, and monocyte chemoattractant protein-1 (MCP-1) in the no-treatment (N), CCR2$^{+/+}$ inflammatory macrophage (I), and CCR2$^{-/-}$ leukocyte (L) groups. Arrowheads indicate disrupted/buried fibrous caps. Scale bar=100 μm. **Bottom**, Quantitation of the number of disrupted/buried fibrous caps, fibrous cap thickness, and Mac3- and MCP-1–positive areas. Data are mean±SEM. *$P<0.05$, **$P<0.01$, and ***$P<0.001$ vs CCR2$^{+/+}$ inflammatory macrophage group. **B**, **Top**, Photomicrographs of the intraluminal surface of the total aorta, stained with oil red O. **Bottom**, Quantitation of the percentage of oil red O–positive area compared with total luminal surface area. Data are mean±SEM. *$P<0.05$ vs CCR2$^{+/+}$ inflammatory macrophage group. **C**, **Top**, Photomicrographs of atherosclerotic plaques in aortic root stained with EVG or Mac3. **Bottom**, Quantitation of plaque size and Mac3-positive areas. Scale bar, 200 μm. Data are mean±SEM. †$P<0.05$ vs CCR2$^{+/+}$ inflammatory macrophage group by 1-way ANOVA followed by Dunnett multiple comparison tests.

Table 1. Characteristics of Brachiocephalic Artery Plaques in the No-Treatment, CCR2$^{+/+}$ Inflammatory Macrophage, and CCR2$^{-/-}$ Leukocyte Groups

	No Treatment (n=9)	CCR2$^{+/+}$ Inflammatory Macrophage (n=5)	CCR2$^{-/-}$ Leukocyte (n=8)
Ruptured plaques per animal, n	3.3±0.2	5.0±0.7†	2.6±0.4
Plaque area, $\times 10^3$ μm^2	230±10	230±10	170±10*
Fibrous cap thickness, μm	1.6±0.2	1.1±0.1†††	2.2±0.3
Lipid core area, %	15±3	20±4	15±3
Macrophage area, %	22±2	32±1**†††	20±3
MCP-1 area, %	21±1	28±2*†	20±3

Data are mean±SEM. Data concerning ruptured plaques per animal were compared by ANOVA followed by Dunn multiple comparison tests. The other data were compared by ANOVA followed by Bonferroni multiple comparison tests. MCP-1 indicates monocyte chemoattractant protein-1.

*P<0.05 vs no-treatment group; **P<0.01 vs no-treatment group;

†P<0.05 vs CCR2$^{-/-}$ leukocyte group; †††P<0.001 vs CCR2$^{-/-}$ leukocyte group.

Immunohistochemical analysis of serial sections revealed that Mac3-positive macrophage infiltration was observed frequently in the shoulder regions of atherosclerotic plaques, and this infiltration was increased in the CCR2$^{+/+}$ inflammatory peritoneal macrophage group compared with the no-treatment group (Figure 1A; Table 1). MCP-1 immunostaining colocalized with macrophages and was also observed in the media. MCP-1 expression in atherosclerotic plaques increased in the CCR2$^{+/+}$ inflammatory macrophage group compared with the no-treatment group, but not in the CCR2$^{-/-}$ leukocyte group (Figure 1A; Table 1). In a subset of experiments, we labeled peritoneal macrophages with PKH26 before adoptive transfer and found that PKH26-labeled peritoneal macrophages were present in the atherosclerotic plaques in the brachiocephalic arteries (Figure IIC in the online-only Data Supplement). In the whole aorta and aortic root, the adoptive transfer of CCR2$^{+/+}$ inflammatory macrophages increased the atherosclerosis area compared with the adoptive transfer of CCR2$^{-/-}$ leukocytes (Figure 1B and 1C), although the serum lipid profile was comparable among the 3 groups (Table I in the online-only Data Supplement).

Measurement of serum biomarkers with a multiplex immunoassay system showed that the adoptive transfer of CCR2$^{+/+}$ peritoneal macrophages, but not CCR2$^{-/-}$ leukocytes, increased the serum levels of MCP-1, MCP-3, and MCP-5, as well as monocyte colony-stimulating factor (Table II in the online-only Data Supplement). Importantly, the adoptive transfer of CCR2$^{+/+}$ inflammatory macrophages increased MMP-9, a metalloproteinase that may degrade the fibrous cap of plaques. Interestingly, the adoptive transfer of CCR2$^{+/+}$ inflammatory macrophages did not affect the serum levels of inflammatory cytokines, such as interferon-γ, tumor necrosis factor-α, and the interleukin family (Table II in the online-only Data Supplement).

Cellular Uptake and In Vitro Kinetics of PLGA Nanoparticles in Macrophages

To clarify the advantage of the nanoparticle-mediated DDS for targeting inflammatory monocytes/macrophages, the cellular uptake and kinetics of PLGA nanoparticles were examined in cultured macrophages. Murine peritoneal macrophages took up FITC-NPs, which were distributed within the cytosol, as detected by confocal microscopy (Figure IVA and IVB in the online-only Data Supplement). Electron microscopy revealed that the PLGA nanoparticles were incorporated into the lysosomes (Figure IVC in the online-only Data Supplement). Cellular uptake of FITC-NP and FITC was quantified as the cellular fluorescent intensity in RAW264.7 cells after a 2-hour incubation with FITC-NP or FITC, followed by a washout period. The FITC signal intensity in cells incubated with FITC-NPs was greater than in cells incubated with FITC over a 7-day period (Figure IVD in the online-only Data Supplement), which suggests that FITC-NP leads to enhanced and sustained uptake in cultured macrophages.

In Vivo Localization of FITC-NPs After Intravenous Administration

Flow cytometric analysis of the blood revealed that neutrophils (36±13%) and monocytes (61±13%) had an FITC signal 2 hours after FITC-NP injection, which suggests that FITC-NPs were taken up through phagocytosis. Flow cytometric analysis of the spleen also revealed the uptake of FITC-NPs in neutrophils and monocytes (Figure 2A). Fluorescence microscopy analysis of the aortic arch and the brachiocephalic arteries revealed the presence of FITC signals mainly in the macrophage areas of atherosclerotic plaques in FITC-NP–injected animals (Figure 2B).

Treatment With Pitavastatin-NPs Inhibits Plaque Destabilization and Rupture

A 4-week treatment with pitavastatin-NPs, but not with FITC-NPs or pitavastatin, significantly reduced the incidence of disrupted/buried fibrous caps associated with thick luminal fibrous caps (Figure 3A; Table 2) and decreased serum biomarkers, including MCP-1, CD40L, vascular endothelial growth factor, and von Willebrand factor (Table III in the online-only Data Supplement). To clarify the pharmacokinetics of nanoparticle treatment, we measured plasma concentration of pitavastatin in the pitavastatin and pitavastatin-NP groups. Plasma concentration of pitavastatin was below the limit of detection (0.625 ng/mL) except 2 hours after intravenous injection of pitavastatin-NP (Table IV in the online-only Data Supplement). There were no significant differences in lipid profiles among the 4 groups (Table V in the online-only Data Supplement). Immunohistochemical analysis revealed that treatment with pitavastatin-NPs attenuated the infiltration of Mac3-positive cells and MCP-1 expression in atherosclerotic plaques (Figure 3A; Table 2). In cultured monocytes, pretreatment with pitavastatin-NPs at 10 μmol/L, but not with pitavastatin at the same dose, inhibited interferon-γ–induced gene expression of MCP-1 (Figure 4B). Consistent with these data, treatment with pitavastatin-NPs, but not FITC-NPs or pitavastatin, decreased the atherosclerosis area in the whole aorta and aortic root (Figure 3B and 3C). Treatment with pitavastatin-NPs, but not with FITC-NPs or pitavastatin, also attenuated the infiltration of Mac3-positive cells to the aortic root (Figure 3C).

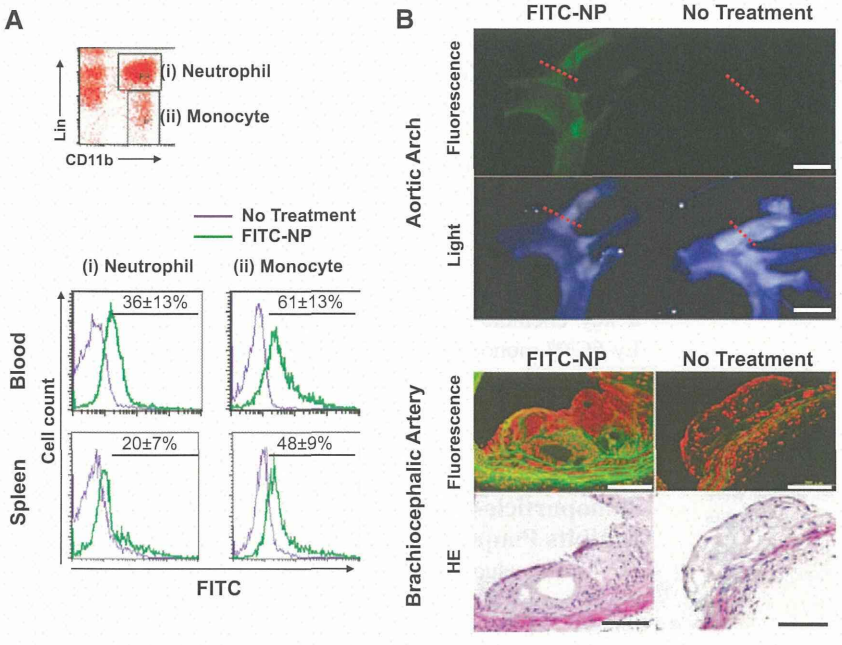

Figure 2. In vivo nanoparticle-mediated drug delivery. **A**, Representative flow cytometry dot plots of circulating leukocytes 2 hours after intravenous injection of PLGA nanoparticles encapsulated with FITC (FITC-NP). Cells were stained with lineage markers and anti-CD11b. The histograms demonstrate FITC uptake by neutrophils (i) and monocytes (ii) in the blood and spleen. Purple indicates control fluorescence in cells derived from uninjected mice. Green indicates fluorescence in cells derived from FITC-NP–injected mice. The percentages of FITC-positive cells is reported as mean±SEM (n=3 per group). **B**, **Top**, Representative fluorescent and light stereomicrographs of isolated segments of the aortic arch 24 hours after intravenous injection of saline (control) or FITC-NPs. Scale bar, 1 mm. **Bottom**, Representative photomicrographs of serial sections of atherosclerotic plaques in the brachiocephalic artery (red dotted line of upper panel) examined with fluorescence microscopy or stained with hematoxylin-eosin (HE). In the fluorescent micrographs, the nuclei were counterstained with propidium iodide (red). Scale bar, 200 μm.

Treatment With Pitavastatin-NPs Inhibits Gelatinase Activity in the Atherosclerotic Plaque

As reported previously, MMP secretion was upregulated in inflammatory monocytes, and focal activation of MMPs is another potential mechanism through which plaques can be destabilized.[33] In situ zymography revealed that pitavastatin-NPs but not control nanoparticles reduced gelatinase activity (Figure 5A). A gelatinase activity

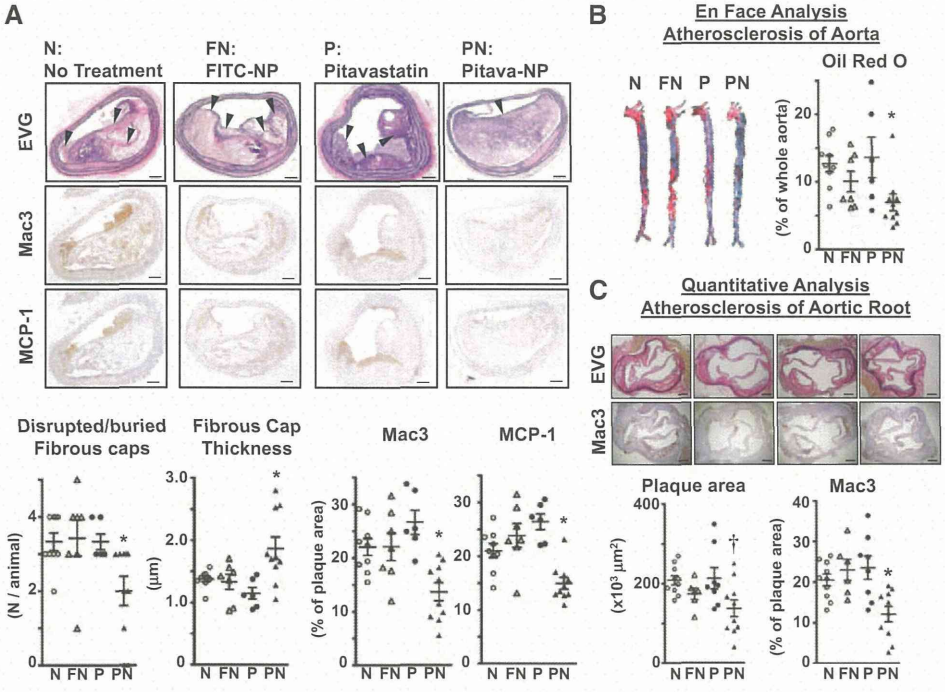

Figure 3. Treatment with nanoparticles (NPs) encapsulated with pitavastatin (Pitava-NP) inhibits atherosclerotic plaque destabilization and rupture. **A**, **Top**, Photomicrographs of atherosclerotic plaques in the brachiocephalic artery stained with elastica van Gieson (EVG), the antimacrophage surface glycoprotein Mac3, and monocyte chemoattractant protein-1 (MCP-1) from the no-treatment (N), FITC-NP (FN), pitavastatin (P), and Pitava-NP groups (PN). Scale bar, 100 μm. **Bottom**, Quantitation of the number of disrupted/buried fibrous caps, fibrous cap thickness, and Mac3- and MCP-1–positive areas. Data are mean±SEM. *P<0.05 vs no-treatment group. **B**, **Top**, Photomicrographs of intraluminal surface of total aorta stained with oil red O. **Bottom**, Quantitation of percentage of oil red O–positive area compared with total luminal surface area. Data are mean±SEM. *P<0.05 vs no-treatment group. **C**, **Top**, Photomicrographs of atherosclerotic plaques in aortic root stained with EVG or Mac3. **Bottom**, Quantitation of plaque size and Mac3-positive areas. Scale bar, 200 μm. Data are mean±SEM. †P<0.05 vs no-treatment group by 1-way ANOVA followed by Dunnett multiple comparison tests. *P<0.05 vs no-treatment group by 1-way ANOVA followed by Bonferroni multiple comparison tests.

Table 2. Characteristics of Brachiocephalic Artery Plaques in the No-Treatment, FITC-NP, Pitavastatin, and Pitavastatin-NP Groups

	No Treatment (n=9)	FITC-NP (n=7)	Pitavastatin (n=6)	Pitavastatin-NP (n=10)
Ruptured plaques per animal, n	3.3±0.2	3.4±0.5	3.3±0.2	2.0±0.4*
Plaque area, $\times 10^3$ μm^2	230±10	170±10	130±40*	150±20*
Fibrous cap thickness, μm	1.6±0.2	1.3±0.1	1.2±0.1	1.9±0.2*
Lipid core area, %	15±3	12±3	8±2	11±2
Macrophage area, %	22±2	22±3	27±2	14±3*
MCP-1 area, %	21±1	24±2	26±2	15±3*

Data are mean±SEM. Data concerning ruptured plaques per animal were compared by ANOVA followed by Dunn multiple comparison tests. Other data were compared by ANOVA followed by Bonferroni multiple comparison tests. MCP-1 indicates monocyte chemoattractant protein-1; and NP, nanoparticles.
*P<0.05 vs no-treatment group.

assay with gelatin zymography in the culture medium of RAW264.7 cells showed that pitavastatin-NPs reduced MMP-9 secretion in a dose-dependent manner, whereas the same dose of pitavastatin showed no effects on MMP-9 secretion (Figure 5B). Both the pro-form and active form of MMP-2 were almost undetectable in the culture medium of RAW264.7 cells, even when stimulated with lipopolysaccharide (Figure 5B).

Treatment With Pitavastatin-NPs Inhibits the Recruitment of Ly-6C^{high} Monocytes to the Circulating Blood

Monocytosis and increased Ly-6C^{high} monocytes in the circulating blood critically promote the progression of atherosclerosis.[31] Treatment with pitavastatin-NP reduced the percentage of monocytes among the total leukocytes on days 7 (Figure 4A). A monocyte subset analysis showed a marked reduction of Ly-6C^{high} monocytes in the circulating blood in the pitavastatin-NP group (Figure 4A). Although CCR2, a key chemokine receptor that promotes the migration of Ly-6C^{high} monocytes, was not affected by pretreatment with pitavastatin-NPs (Figure 4B), MCP-1–induced chemotaxis was inhibited by pretreatment with pitavastatin-NPs in a dose-dependent manner (Figure 4C).

Nanoparticle-Mediated Anti–MCP-1 Gene Therapy Inhibits Plaque Destabilization and Rupture

To further elucidate the impact of inhibition of MCP-1/CCR2 signaling through a nanoparticle-mediated DDS on plaque destabilization and rupture, we examined the effects of nanoparticles that contained plasmids that encode 7ND, a deletion mutant of MCP-1. We previously reported that systemic gene therapy with the 7ND plasmid attenuated the development and progression of atherosclerosis in ApoE$^{-/-}$ mice[27,34–36] and that nanoparticle-mediated transfection of the 7ND plasmid inhibited MCP-1–induced monocyte chemotaxis ex vivo.[37] Treatment with 7ND-NPs reduced macrophage infiltration into the plaques and the incidence of disrupted/buried fibrous caps associated with thick fibrous caps (Figure 6A;

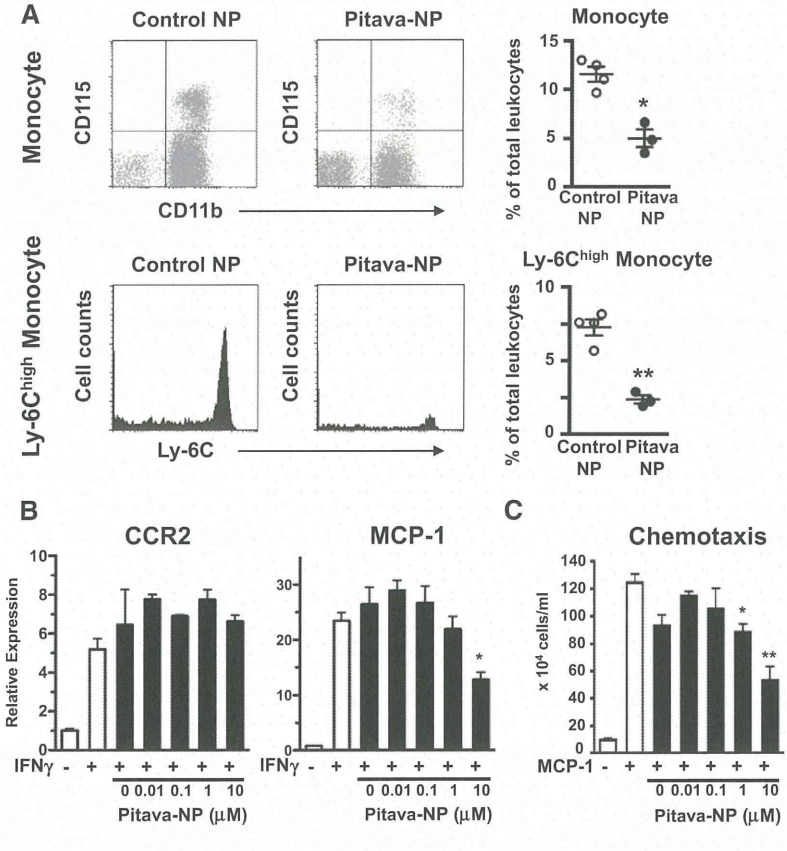

Figure 4. Effects of nanoparticles (NPs) encapsulated with pitavastatin (Pitava-NP) on recruitment of Ly-6C^{high} monocytes. **A, Left,** Representative flow cytometry dot plots and histograms from mice injected intravenously with control (empty) NPs or pitavastatin-NPs. **Right,** Quantitative analysis of ratio of monocytes and Ly-6C^{high} monocytes to total leukocytes is also presented. Data are mean±SEM (n=3–4 per group). *P<0.005 and **P<0.001 vs Control-NP group by unpaired t test. **B,** Effects of pitavastatin-NPs on mRNA levels of CCR2 and monocyte chemoattractant protein-1 (MCP-1) in RAW264.7 cells. Data are mean±SEM (n=3 per group). Data were compared by 1-way ANOVA followed by Bonferroni multiple comparison tests. *P<0.05 vs interferon-γ (IFNγ) group. **C,** Effects of pitavastatin-NPs on MCP-1–induced monocyte chemotaxis in THP-1 cells. Data are mean±SEM (n=3 per group). Data were compared by 1-way ANOVA followed by Bonferroni multiple comparison tests. *P<0.05 and **P<0.001 vs MCP-1 group.

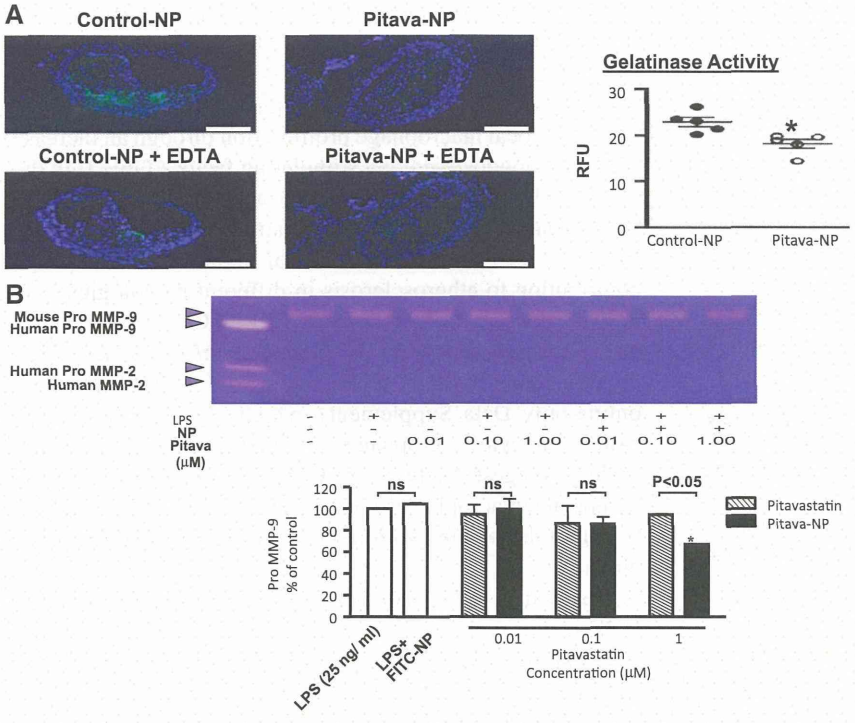

Figure 5. Effects of nanoparticles (NPs) encapsulated with pitavastatin (Pitava-NP) on gelatinase activity of atherosclerotic plaque. **A**, **Left**, In situ zymography for gelatinase activity of atherosclerotic plaque in brachiocephalic artery. Nuclei were counterstained with DAPI. Scale bar, 100 μm. The addition of EDTA was used as a negative control for each section. **Right**, Quantitative analysis of relative fluorescence units (RFUs) of gelatinase activity in atherosclerotic plaques treated with control NPs or pitavastatin-NPs. Data are mean±SEM. *P<0.05 vs Control-NP group by unpaired t test. **B**, Quantitative analysis of native form of matrix metalloproteinase-9 (MMP-9) by gelatin zymography. Data are mean±SEM (n=3 per group) and were compared by 2-way ANOVA followed by Bonferroni multiple comparison tests. *P<0.05 vs lipopolysaccharide (LPS) group by 1-way ANOVA followed by Bonferroni multiple comparison tests.

Table 3), although the serum lipid profile was comparable (Table VI in the online-only Data Supplement). In contrast, treatment with 7ND-NPs did not decrease the atherosclerosis area in the aorta (Figure 6B).

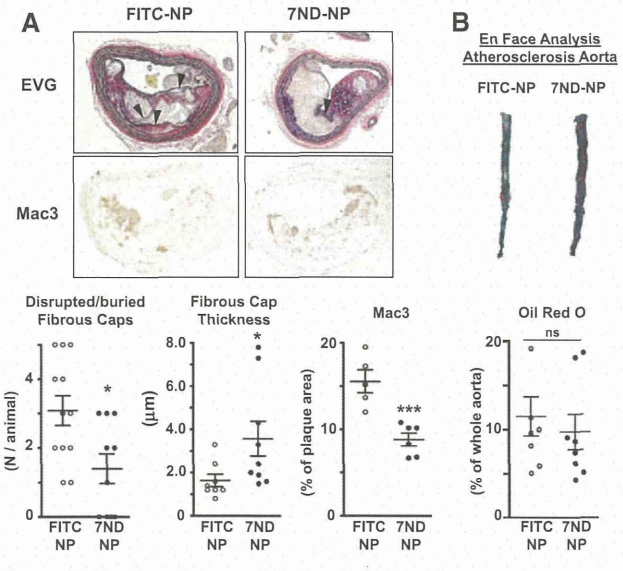

Figure 6. Nanoparticle-mediated anti–MCP-1 (monocyte chemoattractant protein-1) gene therapy inhibits plaque destabilization and rupture. **A**, **Top**, Photomicrographs of atherosclerotic plaques in brachiocephalic artery stained with elastica van Gieson (EVG) or Mac3. Arrowheads indicate disrupted/buried fibrous caps. Scale bar, 100 μm. **Bottom**, Quantitative comparison of number of disrupted/buried fibrous caps, fibrous cap thickness, and Mac3-positive area. Data are mean±SEM. *P<0.05 and ***P<0.001 vs FITC-NP group. **B**, Quantitation of percentage of plaque area compared with total luminal surface area. Data are mean±SEM. There were no statistically significant differences between the 2 groups. FITC-NP indicates nanoparticles encapsulated with FITC, 7ND-NP, nanoparticles encapsulated with 7ND plasmid.

Effects of Oral Treatment With Pitavastatin on Plaque Destabilization and Rupture

Daily oral administration of pitavastatin 0.1 mg/kg had no significant effects on plaque destabilization and rupture, but administration of pitavastatin at 1.0 mg/kg reduced the incidence of disrupted/buried fibrous caps associated with thick fibrous caps and plaque size (Figure VA in the online-only Data Supplement; Table 4). Daily oral administration of pitavastatin 1.0 mg/kg also decreased the atherosclerosis area in the whole aorta and aortic root, whereas administration of pitavastatin 0.1 mg/kg did not (Figure VB and VC in the online-only Data Supplement). Daily oral administration of pitavastatin 1.0 mg/kg significantly inhibited macrophage infiltration and MCP-1 expression in the brachiocephalic artery (Mac3 immunostaining area: 49±3 [$\times 10^3$ μm^2; n=9], 53±5 [$\times 10^3$ μm^2; n=10], and 22±4 [$\times 10^3$ μm^2; n=11] for no treatment, pitavastatin 0.1 mg/kg, and pitavastatin 1 mg/kg, respectively; P<0.01 for no treatment versus pitavastatin 1 mg/kg; MCP-1 immunostaining area: 47±3 [$\times 10^3$ μm^2; n=9],

Table 3. Characteristics of Brachiocephalic Artery Plaques in the FITC-NP and 7ND-NP Groups

	FITC-NP	7ND-NP
Ruptured plaques per animal, n	3.1±0.4 (n=12)	1.4±0.4* (n=10)
Plaque area, $\times 10^3$ μm^2	140±15 (n=8)	170±30 (n=5)
Fibrous cap thickness, μm	1.6±0.3 (n=8)	3.6±0.8* (n=9)
Macrophage area, %	16±1 (n=5)	9±1* (n=6)
MCP-1 area, %	17±2 (n=6)	14±3 (n=6)

Data are mean±SEM. Data concerning ruptured plaques per animal were compared by Mann-Whitney test. Other data were compared by unpaired t test.
MCP-1 indicates monocyte chemoattractant protein-1; and NP, nanoparticles.
*P<0.05 vs FITC-NP.